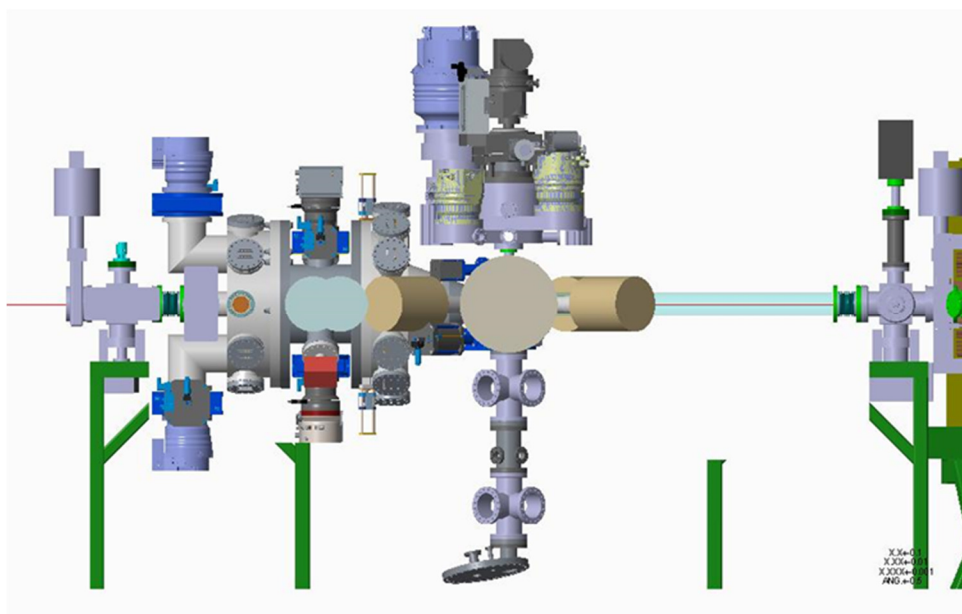


**Technical Report
For the Design, Construction and Commissioning of an In-ring
Spectrometer for Nuclear Reaction Studies at CRYRING**



C.G.Bruno, T.Davinson, C.Lederer-Woods, P.J.Woods
School of Physics & Astronomy, University of Edinburgh, Edinburgh, UK

P.J.Coleman-Smith, M.Cordwell, A.Grant, I.Lazarus, P.Morrall, V.F.E.Pucknell, J.Simpson
STFC Daresbury Laboratory, Daresbury, UK

S.L.Thomas
STFC Rutherford Appleton Laboratory, Chilton, Didcot, UK

D.Seddon
Department of Physics, University of Liverpool, Liverpool, UK

Project Leader/spokesman:

Name: Prof P.J.Woods

E-Mail: p.j.woods@ed.ac.uk

Technical Coordinator:

Name: Dr. T.Davinson

E-Mail: t.davinson@ed.ac.uk

Contact Person at the FAIR site:

Name: Dr. M.Lestinsky

E-Mail: lestinsky@gsi.de

1. Introduction and overview

Hydrogen and Helium burning reactions on radioactive nuclei play a major role in explosive astrophysical scenarios such as novae, X-ray bursts and supernovae. The advent of post-accelerated radioactive ion beams from ISOL facilities has led to significant progress in improving the accuracy of some of these astrophysical reaction rates. However, certain key reaction rates remain largely unconstrained experimentally due to difficulties in producing beams of specific elements with sufficient intensity using the ISOL method. In-flight methods can offer an alternative, but the beam quality is poor and the energies are typically not optimal. A novel approach of using heavy ion beams, decelerated and cooled in-flight in storage rings, pioneered at GSI [1], offers a new approach to this problem. It opens up the potential use of high quality beams of previously inaccessible elements/radioactive isotopes at the energies of interest (\sim MeV/u) [2]. Furthermore, isotopically pure beams can be used to bombard thin, pure targets (avoiding reactions on contaminants such as carbon, *e.g.* see ref.[3]), a particularly important feature in studying astrophysical reactions, while maintaining good luminosity due to the re-circulating beam.

The in-ring spectrometer described in this document has been designed to employ this novel approach at the CRYRING storage ring [4]. Isotopically pure beams, separated in the FRS and decelerated in the ESR, could be injected into CRYRING where they would interact with a high-density gas jet target – see figure 1. Nuclear reaction products could be detected either at very forward laboratory angles for direct nuclear reactions *e.g.* (p, α), or at very backward laboratory angles for indirect measurements *e.g.* (d,p).

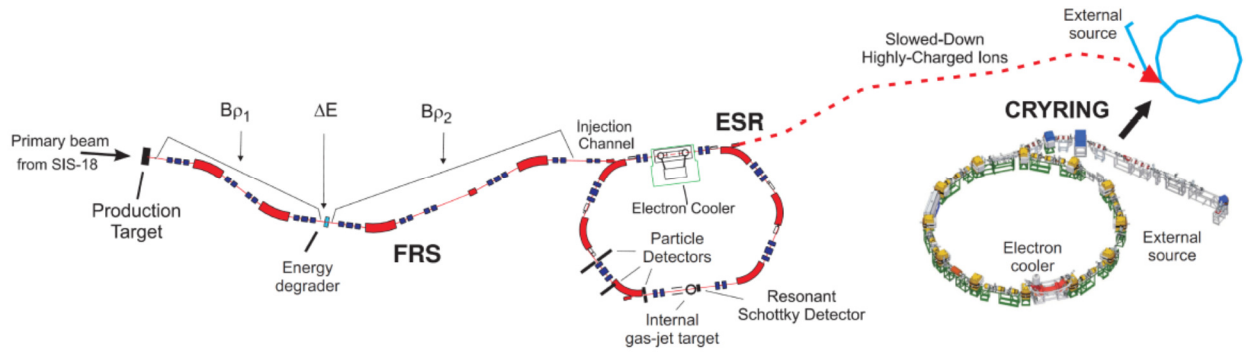


Figure 1: Illustration of radioactive beam production and separation at the FRS, storage and deceleration at the ESR and transfer to the CRYRING.

The first study proposed (experiment S461 submitted to G-PAC43 and rated A-) is the measurement of the $^{30}\text{P}(d,p)$ transfer reaction. This reaction can be used to indirectly probe the ^{31}S compound nucleus populated by the $^{30}\text{P}(p,\gamma)^{31}\text{S}$ nuclear reaction, that plays a key role in Oxygen-Neon (ONe) novae explosions. One classical novae take place in binary systems containing a ONe white dwarf and a less evolved companion star. Hydrogen-rich material from the companion accretes gradually on the ONe white dwarf up to degenerate, unstable conditions eventually leading to a thermonuclear runaway [5]. During the runaway thermonuclear reactions synthesise elements up to calcium [6]. The number of unknown critical reactions required for accurate modelling of novae explosions is small and well defined. The single most important unknown reaction rate is $^{30}\text{P}(p,\gamma)^{31}\text{S}$ which acts as a bottleneck to the production of elements up to calcium (see Figure 2) and is also critical to understand the $^{30}\text{Si}/^{28}\text{Si}$ isotopic ratios observed in pre-solar grains thought to originate from ONe novae. Pre-solar grains are tiny fragments of material, ejected from novae predating the formation of the Solar system, and brought to Earth by meteorites. An improved knowledge of the rate of the $^{30}\text{P}(p,\gamma)^{31}\text{S}$ reaction could allow us to unambiguously identify the type of nova from which a given grain originates.

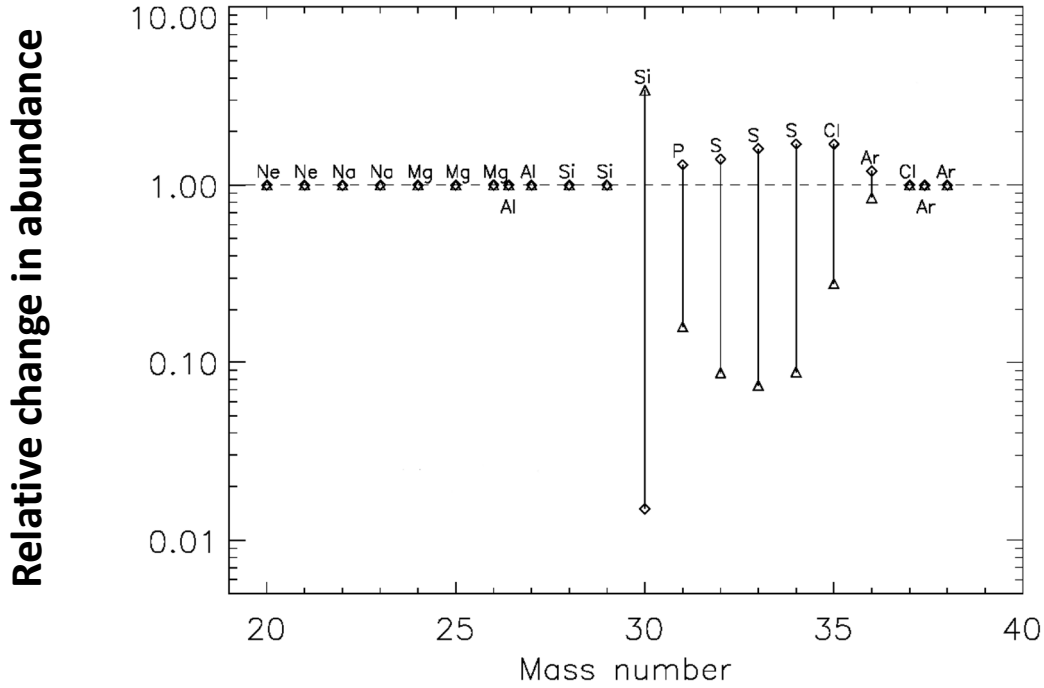


Figure 2: Uncertainties in nova model predictions of the isotopic abundance composition of novae ejecta arising from uncertainties in the $^{30}\text{P}(p,\gamma)$ reaction rate. Adapted from ref. [7].

We would also plan a (d,p) study using a pure isomeric $^{34\text{m}}\text{Cl}$ beam also motivated by nova observations, and (p, α) studies motivated by key reactions in supernovae and X-ray bursts (*e.g.* ^{47}V , ^{59}Cu). In such studies measurements of charged particle reactions could be performed simultaneously with (p, γ) measurements using a zero degree detection system being developed in parallel for CRYRING [8]. This will enable simultaneous measurements between competing compound nucleus decay channels, including inelastic channels such as (p,p'), the latter being important for complete time reverse studies of (α ,p) reactions using the principle of detailed balance [9]. These studies will typically require beam energies from $\sim 3\text{-}6$ MeV/u. Further ahead, we also plan studies utilising the (^3He ,d) proton pick-up reaction to probe resonance strengths in hydrogen burning reactions. The gas jet target system does not presently have ^3He recovery capability, but this could be developed in the future. For the kinematics of (^3He ,d) reactions the chamber can be re-configured for forward angle measurements in the laboratory frame.

2. Physics requirements for subsystem

Nuclear reactions of astrophysical importance are characterised by low angular momentum transfers to specific states within the Gamow window and differential cross section angular distributions which are forward peaked in the centre of mass (CM). The states of interest are typically found at high excitation energy where the density of states is large. Detector systems should therefore be positioned at forward CM angles and have excellent energy resolution.

We propose to study nuclear reactions of astrophysical importance in inverse kinematics. The range of experimental options for studying transfer reactions in inverse kinematics has been well rehearsed elsewhere [9]. For the types of reaction of interest here we note that the high resolution detection of low energy recoiling target-like particle at forward CM angles is possible with a detector system which has excellent energy and angular resolution due to the low rate of kinematic shift.

As an example, we present kinematics and experimental data from the study of the $^{26}\text{Al}(d,p)$ reaction studied in inverse kinematics at 6MeV/u at the ISAC-II facility, TRIUMF [4].

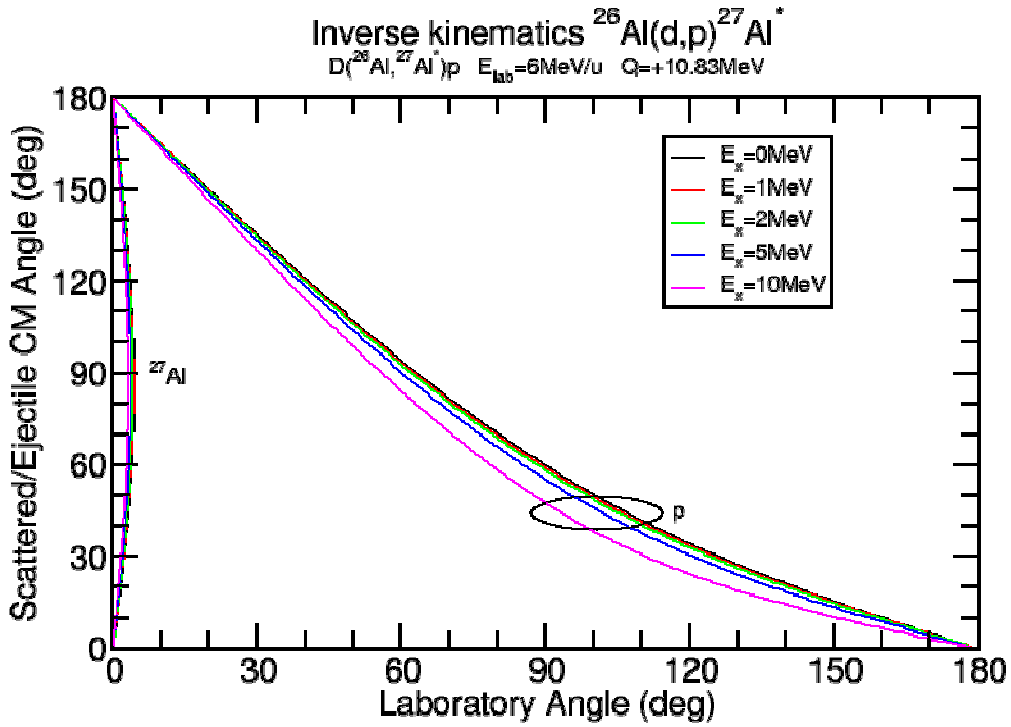


Figure 3: Relationship between CM and laboratory angles for ejectile (^{27}Al) and recoil (p) for the reaction $^{26}\text{Al}(d,p)$ in inverse kinematics. Note that forward CM angles correspond to the detection of the recoil protons at backward laboratory angles.

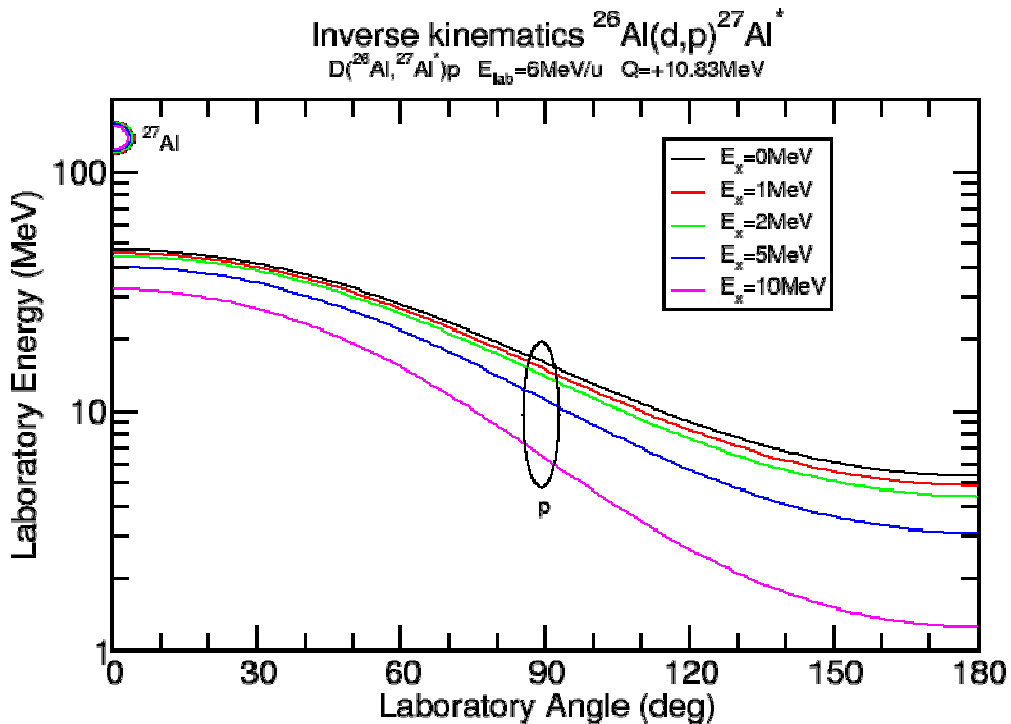


Figure 4: Relationship between laboratory energy and angle for the reaction $^{26}\text{Al}(d,p)$ in inverse kinematics. Note the low kinematic shift for recoil protons at backward laboratory angles and the rapid increase in the kinematic shift at more forward laboratory angles.

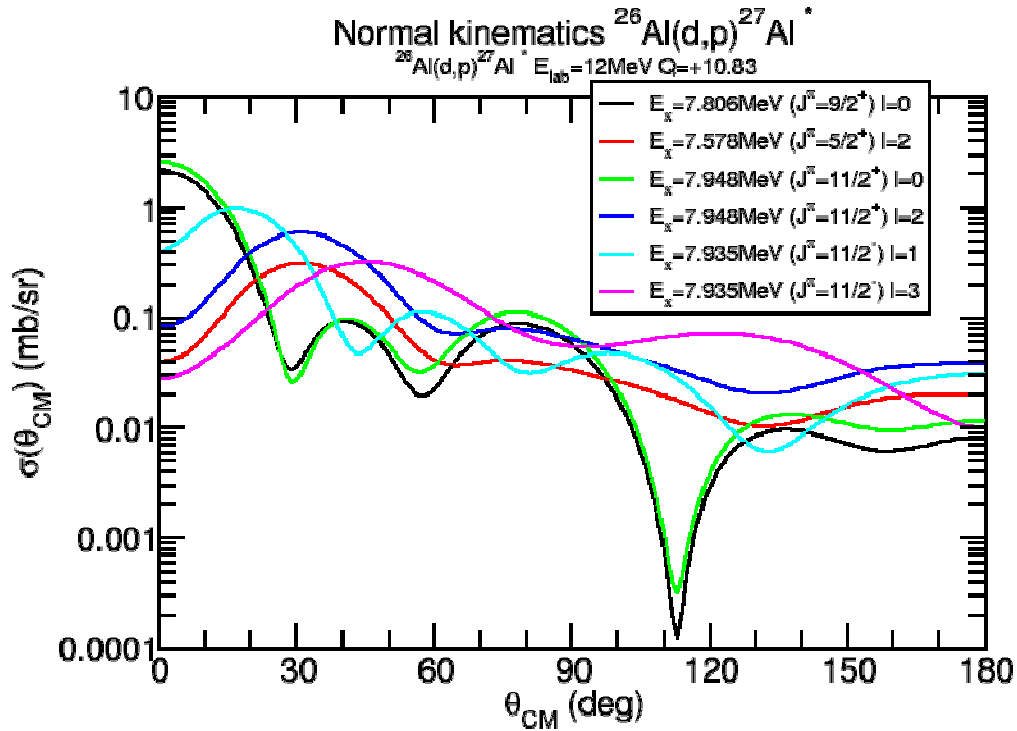


Figure 5: Angular distributions for the reaction $^{26}\text{Al}(d,p)$ illustrating the variation of the laboratory angle of the peak cross section as a function of angular momentum transfer l . Low momentum transfers are forward peaked in the CM frame which corresponds, in inverse kinematics, to the detection of the recoil (p) at backward laboratory angles.

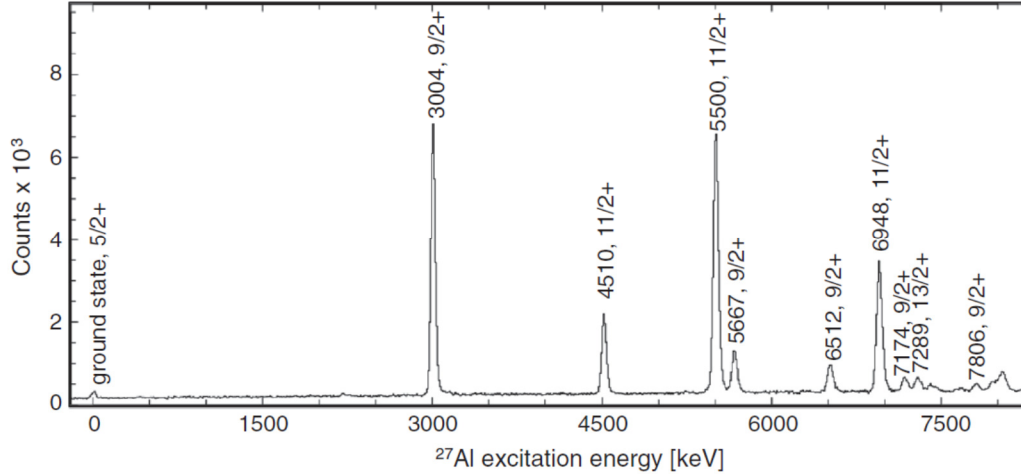


Figure 6: Excitation energy for the reaction $^{26}\text{Al}(d,p)$ in inverse kinematics at 6MeV/u [4].

Figures 3-6 illustrate the inverse kinematics of the $^{26}\text{Al}(d,p)$ reaction and provide an example of experimental data obtained at the ISAC-II facility, TRIUMF at laboratory angles $\sim 160\text{-}179^\circ$. The experimental data has an excitation energy resolution of $\sim 40\text{keV}$ FWHM – the states of astrophysical interest are located at excitation energies $\sim 7.5\text{-}8\text{MeV}$. The excitation energy resolution is dominated (in order) by the electronic noise of the silicon detectors, the energy loss and straggling due to the thin $50\mu\text{g}/\text{cm}^2$ ($\sim 4 \times 10^{18}$ D/cm 2) deuterated polyethylene (CD $_2$) $_n$ target used and the angular resolution of the detector system. The angular resolution of the detector system is determined by the combination of detector size, beam spot size on target and the transverse emittance of the beam. For CRYRING the excellent transverse beam emittance and the use of a narrow width, thin and pure gas jet target means that the excitation energy for such experiments will

be determined by the electronic noise of the detector. It should be noted that the laboratory energies of the protons detected are $\sim 0.5\text{-}5\text{MeV}$ which means that it would not be possible to use the re-entrant pockets with $25\mu\text{m}$ stainless steel windows used at the very much higher energies typical of the ESR.

For indirect studies using transfer reactions e.g. (d,p) , or direct studies e.g. (p,α) or time-reversed (α,p) we will require detector systems at either forward or backward laboratory angles. In some circumstances we will require detector systems at forward *and* backward laboratory angles. To determine the luminosity we will need to observe the characteristic X-rays produced by the interaction the recirculating beam with the gas jet target. This means that we will need X-ray detectors close to the gas jet target.

3. Summary of prototype results

The section provides a *brief* summary of the successful design and development of prototype UHV-compatible silicon detectors and the instrumentation to be used by the in-ring spectrometer for nuclear reaction studies. Further details can be found in section 5.

We developed prototype UHV-compatible double-sided silicon strip detectors (DSSSDs) for the study of the radiative capture reaction $^{96}\text{Ru}(p,\gamma)$ at the ESR, GSI as members of the E108 experiment collaboration. For the first experiment at higher energies [2] the DSSSD was installed in a re-entrant pocket with $25\mu\text{m}$ stainless steel windows. For the second experiment at lower beam energy the DSSSDs were installed in a large bellows section connected to the UHV ESR ring. The DSSSD used is shown in figure 7. Analysis of the second experiment is in progress. From a technical point of view, the prototypes successfully demonstrated the feasibility of using DSSSDs within UHV systems and identified significant improvements to the carrier design and DSSSD operation for future experiments.

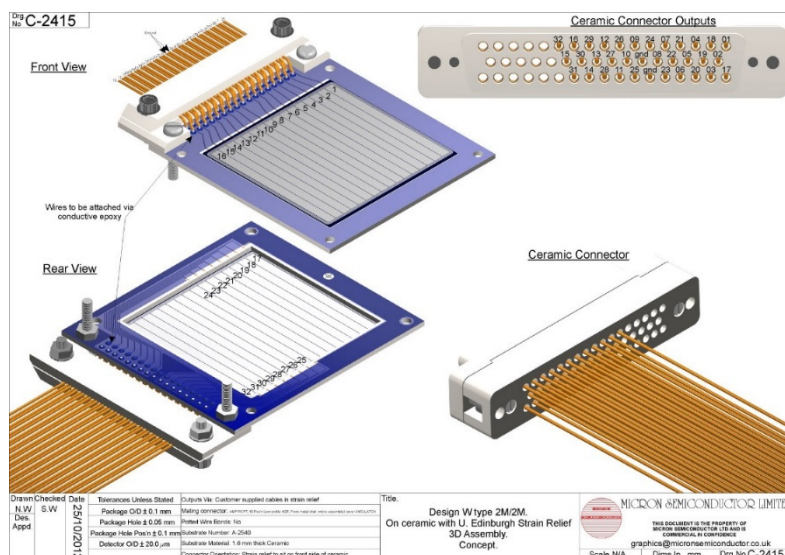


Figure 7: Prototype UHV-compatible DSSSD used for experiment E108 at the ESR.

To instrument the silicon detectors we will use instrumentation developed for the Advanced Implantation Detector Array (AIDA) project. The AIDA collaboration were founding members of the BRIKEN collaboration at the Radioactive Ion Beam Facility (RIBF), RIKEN, Japan. AIDA was installed, tested and commissioned at the BigRIPS separator in 2016 and first experiments commenced in 2017. The test and commissioning phase was used to identify, understand and fix a number of issues with respect to electrical grounding, optimal ASIC settings, FEE64 firmware, data

merger and control interfaces. The AIDA instrumentation system is now operationally robust and reliable.

4. Summary of physics simulations

Performing experiments at CRYRING has a number of advantages with respect to the ESR

- CRYRING circumference $\times 2$ smaller than ESR $\rightarrow \times 2$ higher luminosity
- CRYRING vacuum pressure lower \rightarrow longer beam lifetime
- Longer beam lifetime \rightarrow ESR can prepare next beam cycle during CRYRING measurement for quasi-continuous operation provided radioactive half-life of beam $> \sim 40$ s
- CRYRING expected to provide better low energy beam quality \rightarrow better in-ring spectrometer performance

Calculations were carried out in order to estimate the expected luminosity employing the chamber described in this document. The secondary beam selected in the FRS will be injected into the ESR, stochastically cooled and stacked. This would be followed by deceleration to 30 MeV/u and e-cooling, it would then be decelerated to the energy required at CRYRING followed by further e-cooling. The cooled beam would then be transferred to the CRYRING. At present, the transfer efficiency from the ESR to the CRYRING is not known accurately. We assume that while the measurement is carried out in the CRYRING, a new beam will be prepared in the ESR, to enhance the duty cycle.

For the purposes of illustrating our estimate, we will take the case of the $^{30}\text{P}(d,p)$ reaction (proposal S461, evaluated by G-PAC43 and graded A-). Given the nominal primary beam intensities, the results of LISE++ simulations of the FRS and assuming a 50% transfer efficiency from the ESR to the CRYRING, we expect that around 3.4×10^6 ^{30}P ions ($\tau = 216$ s) could be injected in the CRYRING every 180 s after beam stacking and pre-cooling at 8 MeV/u in the ESR. The beam cycle is illustrated by figure 8.

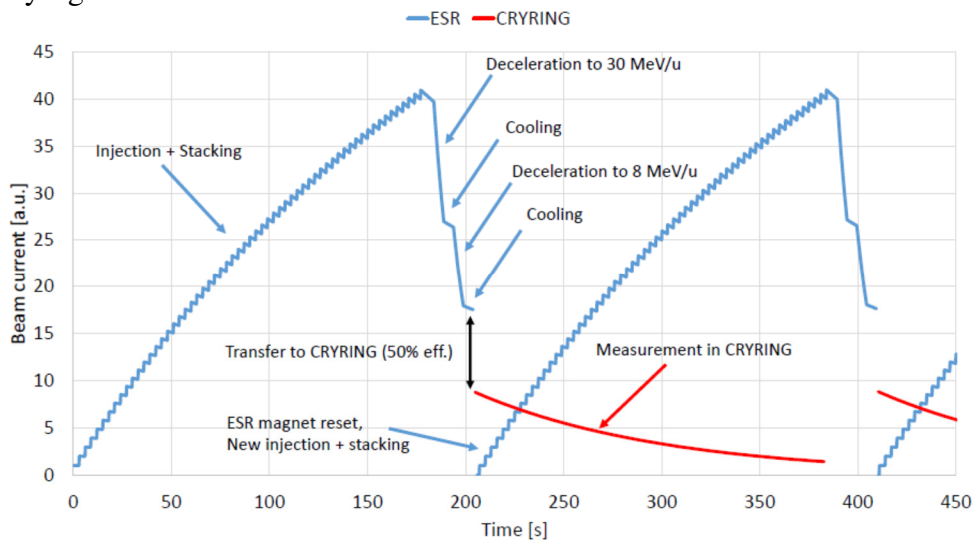


Figure 8: Schematic illustration of the beam cycle for the study of the $^{30}\text{P}(d,p)$ experiment (experiment S461). Injection, stacking and stochastic cooling time can be varied to optimise luminosity. The ESR cooling and CRYRING measurement phases show the radioactive decay time (216s) of the ^{30}P beam.

Once the CRYRING jet gas target is turned on, the beam will interact via electron capture (EC) with the deuterium nuclei of the target. At the energies of interest, the EC cross-section can be written as [1]

$$\sigma = 1.1 \times 10^{-8} \frac{q^{3.9} Z_{\text{gas}}^{4.2}}{E^{4.8}}$$

where σ is the EC cross-section, q is the charge state of the beam, Z is the proton number of the gas the beam interacts with, and E is the energy in keV/u of the beam. At 8 MeV/u, the EC cross-section for ^{30}P beam on a ^2H target is approximately 80 barn. For a realistic target thickness of $n=10^{14}$ atoms/cm², this results in a beam lifetime due to EC of approximately $\tau = 176\text{s}$, which is comparable with the radioactive lifetime of ^{30}P . Note interaction with the residual gas can be shown to be negligible in a UHV environment in this case [11].

One of the advantages of carrying out nuclear physics measurements in a storage ring is the possibility to recirculate the beam after interaction. The “effective target thickness” n_{eff} is a useful figure of merit to determine how effective this technique is compared with traditional solid target measurement. The effective target thickness is defined as the thickness that a traditional solid target would have in order to achieve the same luminosity, and can be computed approximately using [11]

$$n_{\text{eff}} = f n \tau_{\text{EC}}$$

where f is the revolution frequency (700 kHz in this case). Using the numbers provided above one obtains $n_{\text{eff}} = 10^{22}$ atoms/cm², but note this estimate assumes the beam is left to circulate until it completely decays away, which would result in a very low luminosity.

A better estimate can be obtained by dividing the measurement time (180 s in this case) in short time steps (0.2 s), and calculating, time step after time step, the number of surviving beam particles considering both the interaction with the jet target and the radioactive decay. Assuming the beam is refreshed every 180 s, this approach results in $n_{\text{eff}}=6 \times 10^{21}$ atoms/cm² which compares well with typical solid target thicknesses of 10^{17-20} atoms/cm². In particular, it should be noted that high energy resolution requires solid target thicknesses at the lower end of this range – see section 2. The optimal integrated luminosity is approximately 113 1/barn/s. For the S461 proposal to measure the $^{30}\text{P}(\text{d},\text{p})$ reaction the expected counting rate is around 1-10 counts per hour per state. We do not expect any background as the measurement will be carried out at backward laboratory angles. We expect to be able to identify a state with at least 150 counts.

Finally, table 1 reports estimates obtained using the same framework for different measurement conditions at CRYRING. Target species heavier than Helium and beam energies below a few MeV/u result in extremely short beam lifetimes. However, the advantage of using heavy recirculating beams in storage rings over conventional solid target is obvious in most other conditions.

Beam species	Beam energy [MeV/u]	Target species	Target thickness [atoms/cm ²]	EC beam lifetime [s]	Effective thickness [atoms/cm ²]
^{30}P	8	D ₂	10^{14}	176	6×10^{21}
^{30}P	8	D ₂	10^{13}	1763	1×10^{21}
^{30}P	8	D ₂	10^{12}	17630	1×10^{20}
^{30}P	5	D ₂	10^{14}	23	8×10^{20}
^{30}P	2	D ₂	10^{14}	0.45	1×10^{19}
^{30}P	0.5	D ₂	10^{14}	0.001	3×10^{16}
^{30}P	8	^4He	10^{14}	9.6	4×10^{20}
^4He	8	D ₂	10^{14}	5×10^5	2×10^{25}
^{47}V	8	D ₂	10^{14}	33	2×10^{21}

Table 1: Calculated electron capture (EC) beam lifetimes for a selection of beam species, energies, target species, and target energies. The effective thickness is obtained by setting the measurement time to be equal to the shortest between the radioactive lifetime and the EC beam lifetime. The new gas jet target inlet designed by N.Petridis *et al.* (GSI) is designed for densities $<10^{15}\text{cm}^{-3}$ and target widths down to 1mm corresponding to areal densities $<10^{14}\text{cm}^{-2}$.

5. Technical specification and design details

Mechanical design

The single experiment CRYRING experiment section (YR09) (figure 9), the range of the CRYRING experimental programme, CRYRING vacuum requirements and accelerator schedule structure impose the requirement for a modular, multi-purpose (atomic *and* nuclear physics) experiment station. The proposed design is intended to accommodate as many SPARC experiments as possible to maximise operational flexibility.

We have had extended and detailed discussions with Michael Lestinsky (and colleagues) at GSI to understand the requirements of CRYRING@ESR and the in-ring spectrometer. In particular, where to position and how to use the extant X-ray detectors already available at GSI, and how to attach and support the extant CRYRING-supplied gas jet target dump and the new gas jet target inlet provided by other members of the collaboration. Our current design concept envisages the manufacture of two sets of detector chambers (of common design) for upstream and/or downstream silicon detector arrays. Two gas jet target interaction chambers (of different design) would accommodate either detector chambers upstream *and* downstream or, upstream *or* downstream – the latter case would allow other CRYRING collaborators to use part of the YR09 experiment station (figure 10).

These design concepts were presented to the CRYRING@ESR users meeting (March 2017) and the annual CRYRING@ESR meeting (April 2017) to elicit comment and feedback. The design concepts have been further discussed with Michael Lestinsky (and colleagues) at GSI during meetings in June and October. The current design model is illustrated below and has been successfully exported to the GSI in-house CAD/CAE system – also illustrated below. Most of the discussion has focused on the optimisation the X-ray detector configuration around the gas jet interaction chamber (for example angular range, solid angle etc.) and the attachment of the gas jet target inlet and dump to the gas jet target interaction chamber (for example, support frame, accommodation of chamber/beam axis movement, accommodation of chamber thermal expansion during UHV bakeout cycles etc.). The design model observes the design rule of 100mm diameter clearance about the axis of the recirculating beam. This will ensure that uncooled beams can circulate without beam loss.

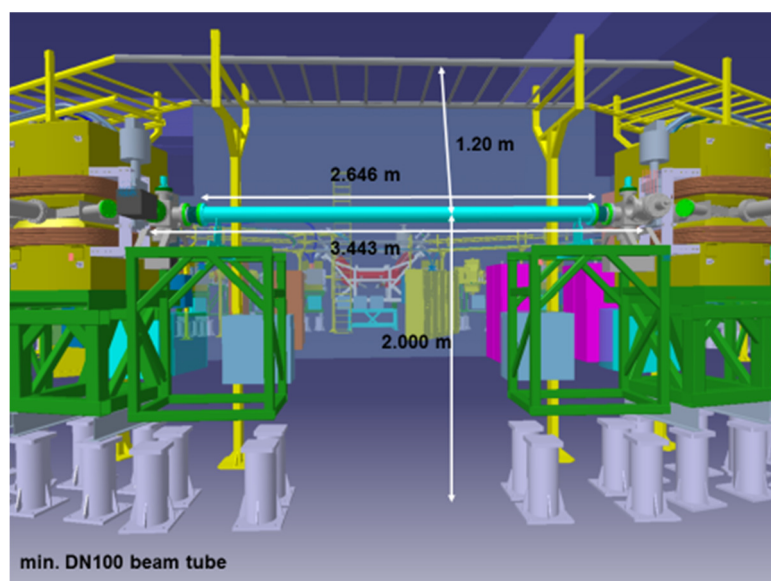


Figure 9: YR09 experiment section of CRYRING. The experiment section can be isolated from the rest of the ring by the gate valves at the ends of the section.

The design of the gas jet interaction chamber provides $\pm 20^\circ$ line of sight upstream and downstream from the silicon detectors to the gas jet target. In-plane ports to which Be windows can be fitted will allow X-ray detectors to view the interaction of the recirculating beam with the gas jet target. X-ray detectors can be positioned at a range of angles: (internal radius 5, 20, 54.7, 90, 120, 160 and 175° , external radius 5, 20, 54.7, 90, 120, 160 and 175°) but cannot be positioned closer to the beam axis than $\sim 5\text{cm}$ radius to avoid stopping uncooled beams.

FLANGE ANGLE	DISTANCE (mm)	FLANGE SIZE	CORRESPONDING DRAWING	DETECTOR TYPE
$\pm 5^\circ$	785	DN 100	NP70-01-2120	EGSP-52x30-12-5-N SIDE VIEW
$\pm 20^\circ$	675	DN 100	NP70-01-2120	EGSP-52x30-12-5-N SIDE VIEW
$+45^\circ$	178	DN 40	NP70-01-2480	ORTEC GLP CFG-PG4
$+90^\circ$	222	DN 160	NP70-01-2480	Julich X-Y Si(Li)
$+135^\circ$	178	DN 40	NP70-01-2480	ORTEC GLP CFG-PG4
-54.7°	147	DN 40	NP70-01-2480	ORTEC GLP CFG-PG4
-90°	196	DN 63	NP70-01-2480	ORTEC GLP CFG-PG4
-120°	159	DN 40	NP70-01-2480	ORTEC GLP CFG-PG4

Table 2: Summary of the in-plane gas jet interaction chamber flanges to be used with the extant X-ray detectors available at GSI. Quoted distances are from the gas jet target to the the front the detector cryostat. Chamber internal diameter 189mm. Note that the use of Eurisys side view X-ray detectors at $\pm 5^\circ$ and $\pm 20^\circ$ requires the use of an ESR bellows-mounted DN100 re-entrant pocket with Be windows.

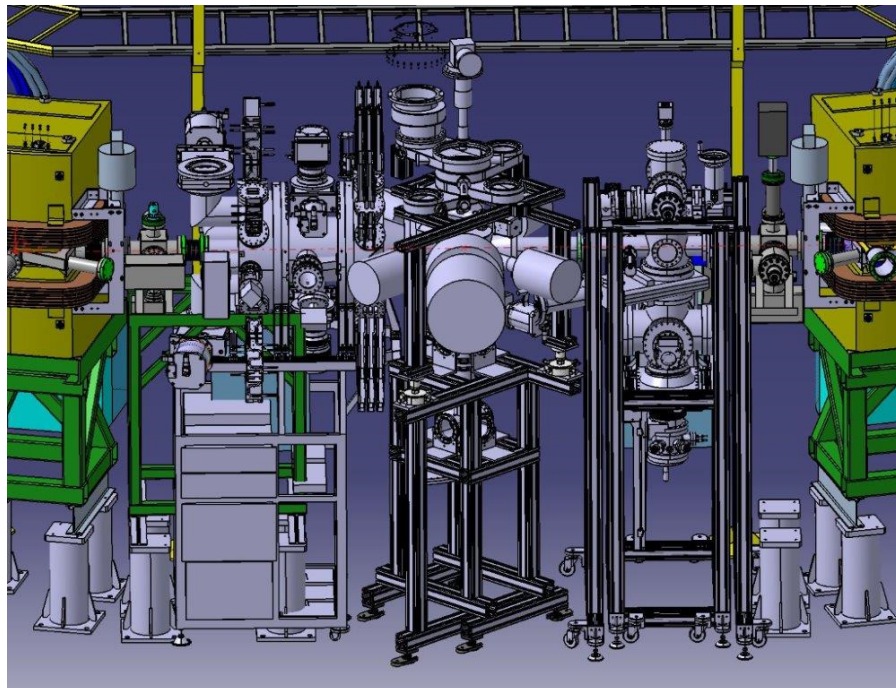


Figure 10: Image of the CRYRING YR09 experiment section from the CATIA CAD/CAE package used at GSI. It illustrates the integration of the (in this case, upstream – left hand side) in-ring spectrometer detector chambers, (middle) gas jet interaction chamber and (downstream - right hand side) electron target to be used by other CRYRING collaboration members for atomic physics electron-ion interaction experiments.

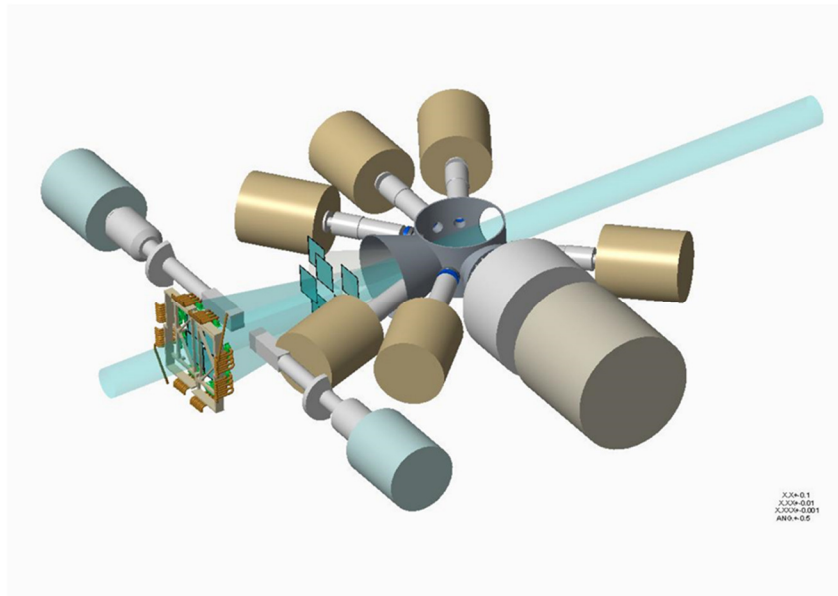


Figure 11: Example of design concept. Central interaction chamber for GSI gas jet target with multiple ports with Be windows for X-ray detectors. Currently there are 4× Ortec X-ray detectors (six are shown to illustrate potential mechanical conflicts), 2× Eurisys 30mm × 50mm, segmented, side-windowed X-ray detector and 1× Julich x-y segmented Si(Li) X-ray detector available at GSI. The Eurisys X-ray detectors can be positioned at $\pm 5^\circ$ and $\pm 20^\circ$ using standard bellows-mounted, GSI re-entrant vacuum pockets with Be windows. Also illustrated are 4× 10cm × 10cm and 8× 10cm × 10cm silicon DSSSDs at ~900mm and ~450mm upstream from the gas jet target. The DSSSDs furthest upstream need to move towards and away from the beam axis with the beam cooling cycle. The DSSSDs nearest the target do not need to move with the beam cooling cycle.

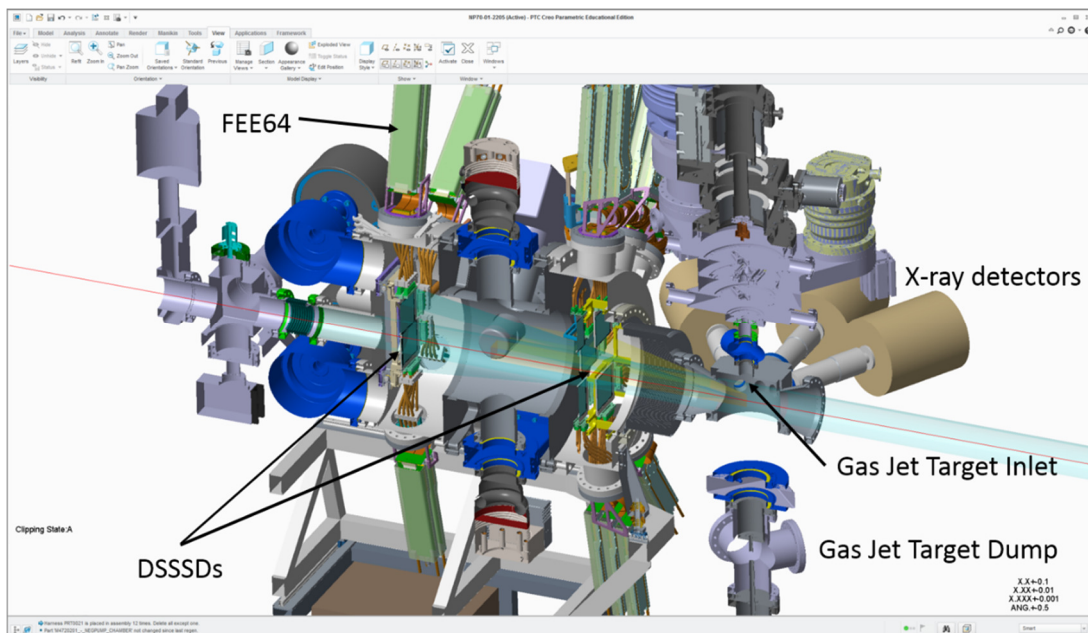


Figure 12: Cross section of UHV detector chambers, gas jet interaction chamber, gas jet target inlet and dump, and support frame.

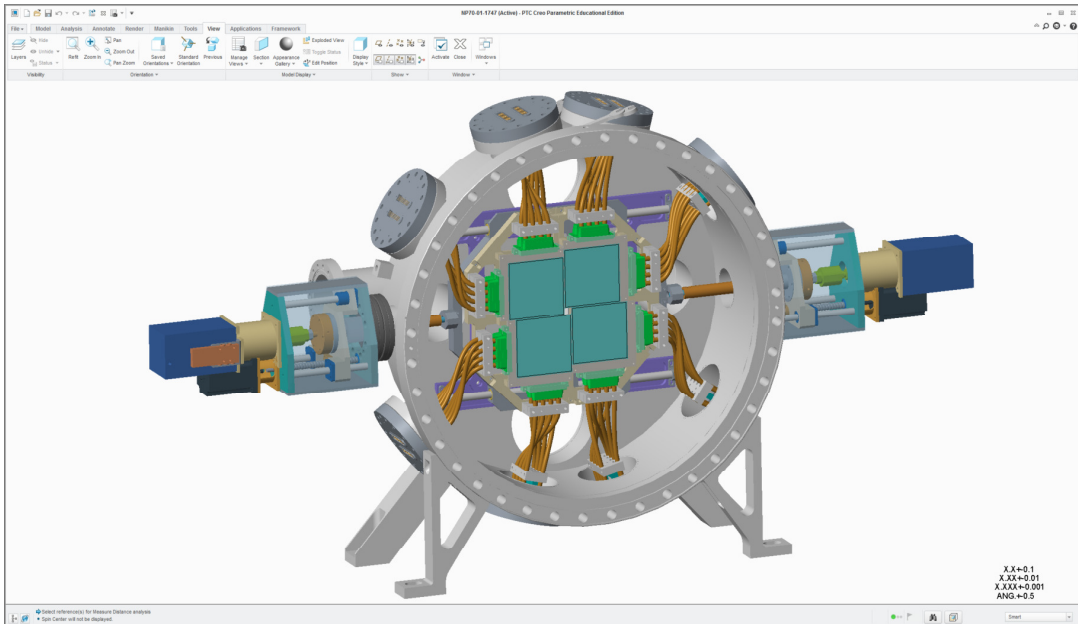


Figure 13: UHV detector chamber for detectors ~900mm from gas jet target. These detectors have to be positioned $\pm 5\text{mm}$ about the beam axis to detect recoils at very backward, or recoils/ejectiles at very forward, laboratory angles. These detectors have to be moved using stepper motors and linear translators to $\pm 5\text{cm}$ about the beam axis during beam injection and cooling or, when not in use. The $4 \times 10\text{cm} \times 10\text{cm}$ DSSSDs are transversely and longitudinally offset to avoid mechanical conflicts.

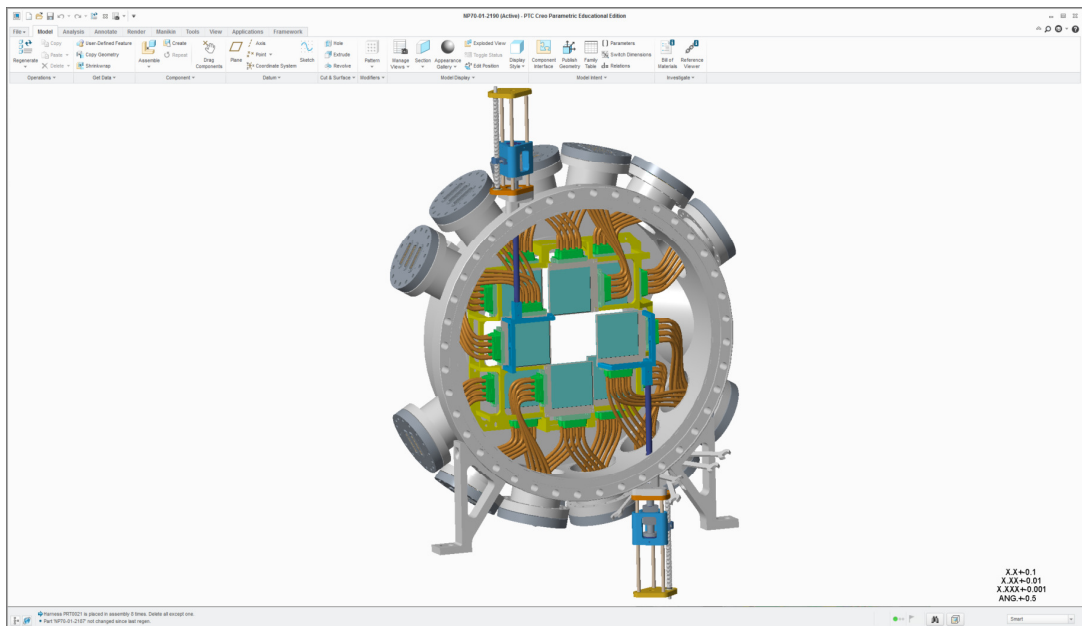


Figure 14: UHV detector chamber for detectors ~450mm from the target. Up to $8 \times 10\text{cm} \times 10\text{cm}$ DSSSDs can be arranged around a central $10\text{cm} \times 10\text{cm}$ opening providing line of sight to the other detector chamber (figure 13). The DSSSDs are longitudinally offset to avoid mechanical conflicts.

Gas jet target

CRYRING will use the new gas jet target inlet designed by N.Petridis *et al.* (GSI) and the extant CRYRING gas jet target dump. The design model of the gas jet target inlet and dump have been incorporated into our design model. SPARC will be responsible for the design and construction of

the support frame for the gas jet target inlet and dump. The gas jet target will be the subject of a separate technical design review (TDR) and will not be discussed further here.

Alignment

All major elements of CRYRING have multiple attachment points for 1.5 inch spherical reflectors which are used for alignment using laser-based theodolites. The detector and gas jet target interaction chambers will also use this method of alignment.

Vacuum

The STFC Daresbury Laboratory vacuum group have simulated (Molflow) the vacuum performance of the detector and gas jet target interaction chambers using the mechanical design model to generate a model of the internal surfaces of the chambers (figure 15). The model assumes vacuum-fired stainless steel construction with an outgassing rate of 1×10^{-13} mbar.l/s/cm² and a pumping speed of 1200 l/s.

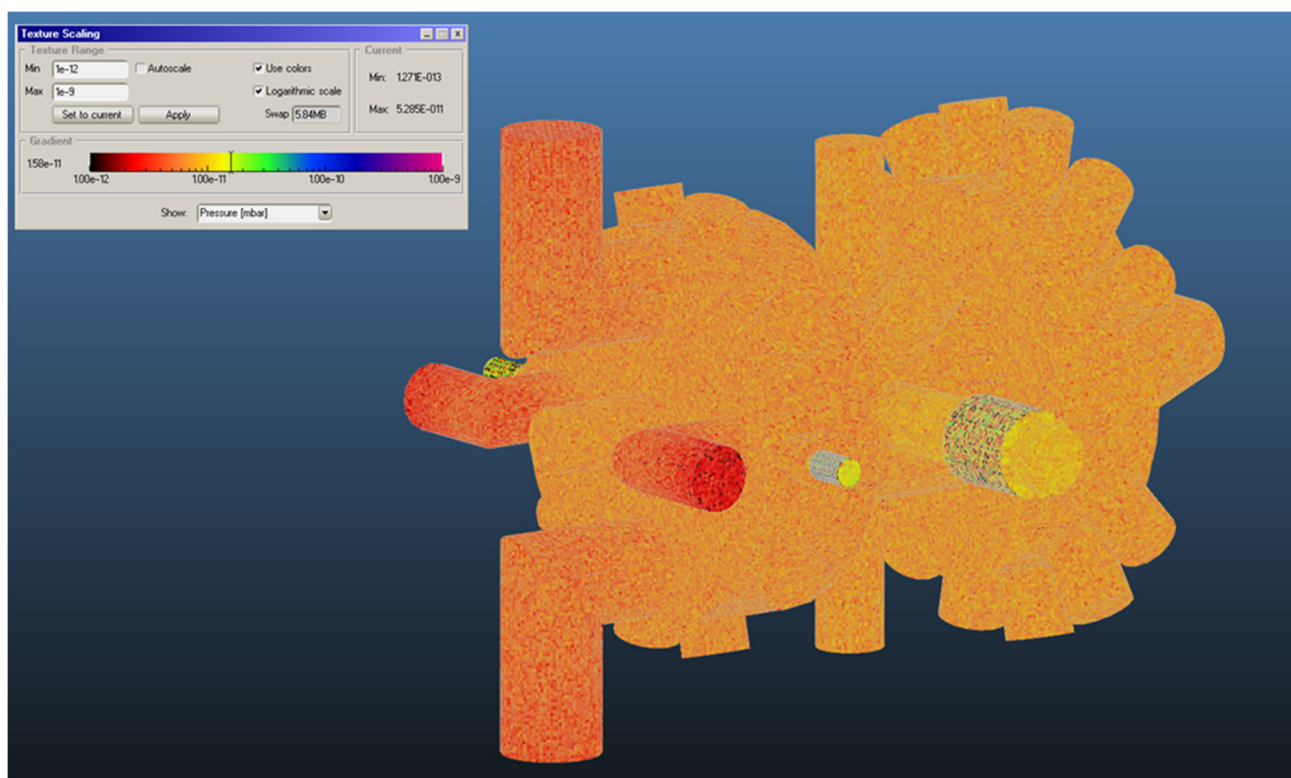


Figure 15: Vacuum model of the interior volume of the detector and gas jet interaction chambers. The model indicates that it is possible to achieve $\sim 1\text{E-}11$ mbar with an empty chamber and 1200l/s pumping speed.

Double-sided silicon strip detectors (DSSSDs) will be installed in the detector chambers. The detector silicon wafer will be supported by a ceramic carrier. Individual strips of the DSSSD will be connected to gold traces on the ceramic carrier via ultrasonically-bonded 25 micron aluminium wires. Cables from the DSSSDs to the vacuum signal feedthroughs will be electrically connected to the ceramic carrier by (minimal) quantities of a UHV-rated silver-loaded epoxy and mechanically secured by a ceramic strain relief.

The cables will be constructed from silver-plated copper wire and wrapped by UHV-rated heat-treated Kapton type F film. The cables will be terminated by crimp sockets which will housed within

a MACOR 78-pin D-connector. The 78-pin D-connectors will be connected to dual 78-pin D-connector UHV vacuum feedthroughs.

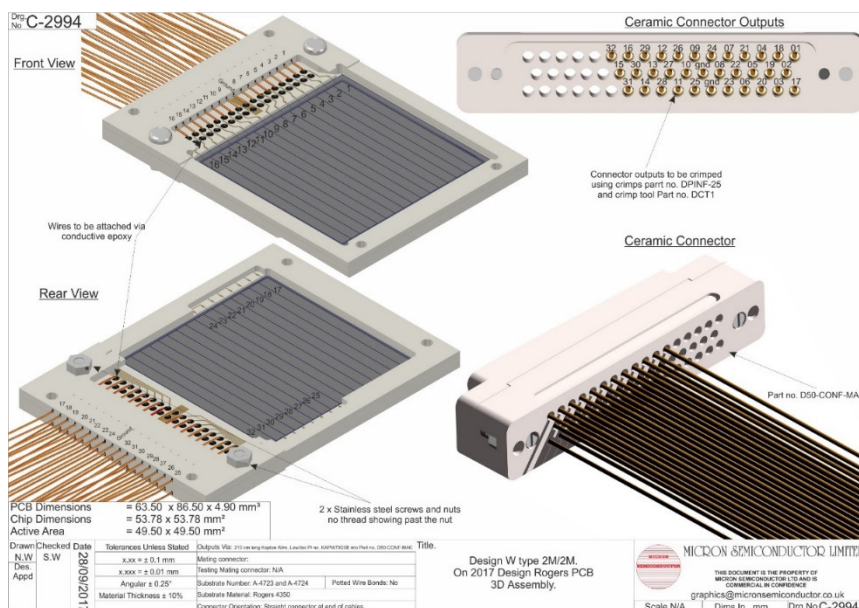


Figure 16: Manufacturer’s assembly drawing for UHV-compatible MSL type W DSSSD illustrating ceramic carrier and strain relief, 32 × 2.1m Kapton cables and MACOR D-connector. Two of these DSSSDs will be used for experiment E127 at ESR and CRYRING.

The vacuum chamber specification assumes 316L construction as a minimum with 316 LN flanges. All vacuum chambers will be vacuum fired to 950° C for 2-4 hours. We will use a combination of turbo, ion and neg vacuum pumps to achieve the required pumping speed. The overall pumping capacity to be installed will be determined by the outgassing load which is expected to be dominated by the Kapton cabling. This is currently being evaluated experimentally at the STFC Daresbury Laboratory with an XUHV test chamber and will be used to specify the required system pumping speed. The required vacuum performance will be demonstrated during commissioning. We will observe the CRYRING practice of installing gate valves between turbo pumps and the ring.

The UHV chambers will be fitted with a custom, removable jacket with integrated heating elements and thermal insulation for bakeout. Vacuum chamber ports will use heating collars. All vacuum chambers will be fitted with appropriate vacuum gauges. To minimise system integration issues we expect to adopt extant CRYRING standards for vacuum controllers, gauges, manifolds for bakeout d.c. power and type K thermocouples etc.

Detectors

We will use 10cm × 10cm, 128 × 128 double-sided silicon strip detector (DSSSD) with wafer thicknesses of 500µm or 1000µm and integrated poly-silicon 10M bias resistors. Detectors of this size and type have been supplied commercially for more than five years – the technology is well-established. The strip pitch of ~750µm will provide the necessary angular resolution for DSSSDs positioned at ~450mm and 900mm from the gas jet target. The silicon wafer will be mounted in a ceramic transmission carrier using (small quantities) of a UHV-rated silver-loaded epoxy glue. Individual strips will be electrically connected to gold contact pads on the carrier by ultrasonic wire bonds. Traces from the contact pads will connect the strips to the cabling between the DSSSD carrier and the vacuum chamber signal feedthroughs.

Instrumentation

The Advanced Implantation and Decay Array (AIDA) [12] was developed to support DESPEC experiments at FAIR. An AIDA system was installed and commissioned at BigRIPS, RIBF, RIKEN in 2016 and an experimental program commenced 2017. The manufacture of AIDA hardware for CRYRING is complete. Commissioning tests have been completed.

An application specific integrated circuit (ASIC) was developed for AIDA. The ASIC has 16 channels with two sets of preamplifiers, shaping amplifiers and discriminators per channel. One preamplifier has selectable sensitivity (20MeV or 1GeV FSR), the other preamplifier has a sensitivity of 20GeV FSR and is enabled only if the energy observed by the other preamplifier exceeds a defined threshold value. Peak analogue outputs from the shaping amplifier are held and readout via a multiplexor. Four ASICs are grouped on an ASIC mezzanine PCB. The ASIC mezzanine PCB is connected to a front end electronics card (FEE64). The FEE64 provides 4×16 -bit, 1MHz ADCs to digitize the multiplexed ASIC outputs. The FEE64 integrates the readout, ASIC control, data acquisition and user interface with a Xilinx Virtex 5 FPGA with an integrated PowerPC CPU running Linux. Each FEE64 is therefore an autonomous 64-channel signal processing and data acquisition system. To synchronise data from different FEE64s a 100MHz, 48bit timestamp is distributed from a master FEE64 to all other FEE64s.

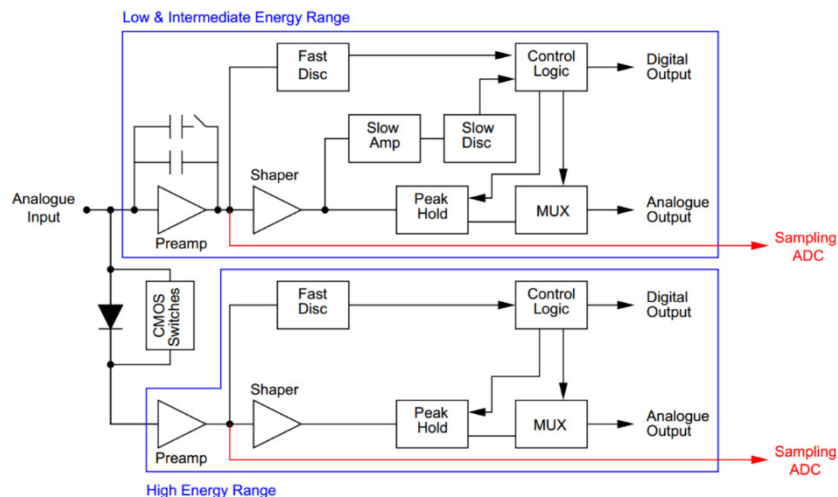


Figure 17: Schematic diagram of the functionality of one ASIC channel.

Each FEE64 has a system console serial port, RJ45 GBit network port, HDMI timestamp port and a power connector. Data from the FEE64 is routed by a network switch to a server where a merger program merges data from all FEE64s into a single, time-ordered data stream using the GREAT Total Data Readout (TDR) format.

At RIKEN it is necessary to use long cables (c. 100cm) between the DSSSDs and ASICs so the electronic noise is dominated by the capacitance of the cabling and approximately linearly related to the length of the cabling. We typically obtain an electronic noise of 50keV FWHM for the 20MeV FSR setting with a 5σ slow comparator threshold of ~ 105 keV. At CRYRING the cable lengths will be ~ 30 cm and we expect to achieve an electronic noise of ~ 15 -20keV FWHM for the 20MeV FSR setting.

STFC Daresbury Laboratory is developing new firmware to support the distribution of the GSI variant of the White Rabbit timestamp and has delivered a demonstrator system to GSI for test and evaluation in December 2017. It will therefore be possible to integrate the AIDA data acquisition with other data acquisition systems whether they are able to use White Rabbit, or not.

We have manufactured 32× FEE64s (plus spares) plus the necessary support infrastructure. This is sufficient to support systems of up to 2048 channels or 8× 128×128 DSSSDs.

6. Radiation environment, safety issue

The detector system will be used with low intensity, low energy radioactive ion beams within the CRYRING experimental hall to which there will be no access during when is beam is on. The detectors and interior surfaces of the vacuum chambers should only be exposed to scattered beam or reaction products and hence short-lived or accumulated radioactivity should be at a low level. If the chambers are to be opened following beam delivery wipe tests should be performed to confirm that there is no measurable radioactive contamination.

Other possible hazards not specific to the detector system include detector and instrumentation power supplies, hot surfaces during bakeout, mechanical hazards etc. These will be identified, assessed and safe working practices adopted.

7. Production, Quality Assurance and Acceptance Tests

The DSSSDs will be undergo standard *V-I*, pulser and radioactive source tests upon delivery.

The production and acceptance tests for AIDA instrumentation hardware are complete. The development of new firmware to support the GSI variant White Rabbit timestamp is complete with a demonstrator system has been delivered to GSI in December 2017 for test and evaluation.

The detector and gas jet target UHV chambers will be assembled at STFC Daresbury Laboratory upon delivery. The chambers will be vacuum tested (without load and with blank flanges) to verify the expected vacuum performance. When successfully completed, feedthrough flanges and a realistic outgassing load will be installed and vacuum tested to demonstrate that we can meet CRYRING vacuum standards.

8. Calibration (if needed) with test beams

An approximate energy calibration of the detector array can be obtained from a pulser walkthrough to determine the ADC offset and the $\pm 3\%$ tolerance of the 0.7pF charge sensitive preamplifier feedback capacitor (20MeV FSR). This basic energy calibration can be checked by extended data collection runs (~7 days) to obtain alpha energy spectra from background events from the Uranium $4n+2$ decay series.

In most cases it will be possible to obtain a precise, internal energy calibration by using the experimental data, for example, from strongly populated ground and low-lying excited states in (d,p) reactions. In some circumstances, for example where the luminosity is expected to be low, we would plan to use a higher intensity isobaric beam during an experiment to obtain a precise energy calibration.

9. Civil engineering, cave, cooling, cranes etc.

Electrical power

We will require single- and three-phase ac electrical power. Most of the equipment to be installed will use single-phase ac electrical power. Based on experience with AIDA@RIKEN the EDAQ hardware will require ~15A. We expect that the vacuum hardware will require a similar amount of power.

The AIDA FEE64s need to be water-cooled and we will use a Julabo FL11006 recirculating chiller and a set point of +20° C to provide the cooling required. The Julabo FL11006 uses 400V/3PNPE/50Hz (V/Hz 360-440/3PNPE/50, current input at 230V of 17A) or 230V/3PPE/60Hz (V/Hz 197-242/3PPE/60, current input at 230V of 27A). The Julabo FL11006 is air-cooled and can provide a maximum of 11kW of cooling at +20° C and typically operates at ~3-4kW with typical AIDA FEE64 configurations. The preferred coolant is tap water.

Network

We will need two, dedicated network cables (Cat6 for distances to 100m, or fibre for distances >200m) from the experimental hall to the experiment counting/control room. These will be connected to 2× 24-port, Gbit network switches in the experimental area and to an additional, multi-port Gbit network card in the data acquisition computer in the experiment counting/control room. Experimental data from each FEE64 will be received by the data acquisition computer where it will be merged to form one, time-ordered data stream and written to disk. The network will also be used to connect to several Raspberry Pi computers in the experimental area which will be used to control ac mains power to the AIDA FEE64s, FEE64 system consoles, 4× CAEN N1419 detector bias modules and the Julabo FL1006 recirculating chiller via USB or serial-USB links.

Space

In addition to the detector and gas jet target chambers we will require space for one 19” rack and the Julabo FL11006 (W×L×H 78cm ×85cm ×148cm, weight 250kg). The 19” rack will house 2× 1U 24-port, Gbit network switches, 4× 3U AIDA FEE64 PSUs, 2× 7U NIM bins and 2× 3U USB-controlled ac mains relay. The hoses and electrical cables from the 19” rack and Julabo FL11006 to the AIDA FEE64 hardware will have a length ~5m. The Julabo FL11006 and 19” rack can be moved from the vicinity of the YR09 when not in use. Space will be required for the storage of the Julabo FL11006, 19” rack and unused vacuum chamber sections when not in use.

Temperature & Humidity

The experimental equipment should be able to operate without problem in the temperature range from ~15-40° C. AIDA@RIKEN has operated without problem at relative humidities from 20-50%. The Julabo FL11006 chiller is typically operated at +20° C and *always* above the dew point.

Crane

The detector and gas jet target support stands, 19” rack and Julabo FL1006 will all have wheels to facilitate installation and removal from YR09. It may be necessary to lift vacuum chamber elements or assemblies of chamber elements onto the support stand which would require the lift of up to 500kg.

10. Installation procedure, its time sequence, necessary logistics from A to Z including transportation

Upon the successful completion of acceptance and commissioning tests at the STFC Daresbury Laboratory we will arrange for the shipment of all equipment to CRYRING. The process of installation at CRYRING will necessarily depend upon the scheduled activities of CRYRING and we will seek to minimise the impact on other CRYRING operations. Assuming that access to YR09 is possible, we would plan to install and align the detector and gas jet target interaction chamber assembly at YR09. Once aligned, we would plan to align and attach the gas jet target inlet and dump

to the gas jet interaction chamber. At this stage we could proceed to commissioning tests to demonstrate the vacuum performance of the assembled system with an operational gas jet target.

11. Cost and funding

This project is fully funded by a UK Science Technology Facilities Council (STFC) grant ST/M001652/1 *ISOL-SRS: ISOL Beam Storage Ring Spectrometer* for the period from January 2015 to March 2019. The grant includes funds for equipment, travel and UK manpower to design, manufacture, assemble and test the silicon detectors, instrumentation and vacuum systems. This project represents one workpackage (WP2) of the overall STFC PPRP grant *ISOL-SRS: ISOL Beam Storage Ring Spectrometer* which was awarded to a collaboration of the University of Edinburgh, University of Liverpool and the STFC Daresbury Laboratory. The project costs will form part of the overall UK contribution to FAIR experiments.

12. Organization and distribution of responsibilities

STFC PPRP grant *ISOL-SRS: ISOL Beam Storage Ring Spectrometer* is organised as follows:

Spokesperson	P.J.Woods, University of Edinburgh
Technical Co-ordinator	I.Lazarus, STFC Daresbury Laboratory
Project Manager	M.Cordwell, STFC Daresbury Laboratory
WP2 Project Manager	T.Davinson, University of Edinburgh

Mechanical design, electronics and software engineering support is provided by STFC Daresbury and Rutherford Appleton Laboratories.

References

- [1] B. Mei *et al.*, Phys. Rev. C **92** (2015) 035803
- [2] M. Lestinsky *et al.*, Eur. Phys. J. Special Topics **225** (2016) 797
- [3] V. Margerin *et al.*, Phys. Rev. Lett. **115** (2015) 062701
- [4] *Physics book: CRYRING@ESR*
M.Lestinsky *et al.*, (2016) European Physical Journal: Special Topics, **225** (5), pp. 797-882
<http://dx.doi.org/10.1140/epjst/e2016-02643-6>
- CRYRING@ESR: A study group report*
M.Lestinsky *et al.*
https://www.gsi.de/fileadmin/SPARC/documents/Crying/ReportCrying_40ESR.PDF
- Low Energy Storage Ring Technical Design Report version 1.3*
H.Danared *et al.*
http://www.fair-center.eu/fileadmin/fair/publications_exp/DesignReportLSR_1.3.pdf
- [5] S. Starrfield, C. Illiadis and W.R. Hix, Pub. Astron. Soc. Pac. **128** (963) (2016) 051001
- [6] J. José and M. Hernanz., J. Phys. G Nucl Part. Phys. **34** (2007) R431

- [7] C. Illiadis *et al.*, *Astrophys. J. Suppl. Ser.* **142** (2002)
- [8] Technical Design Report: Experimental Instrumentation of CRYRING@ESR
Z. Andelkovic *et al.*
http://www.fair-center.eu/fileadmin/fair/publications_exp/TDR_CRYRING_Experimental_Instrumentation.pdf
- [9] P. Salter *et al.*, *Phys. Rev. Lett.*, **108** (2012) 242701
- [10] J.S.Winfield, W.N.Catford and N.Orr, *NIM* **A396** (1997) 147
- [11] M. Grieser *et al.*, *EpJ Special Topics* **207**(1) (2012) 1
- [12] AIDA: A 16-channel amplifier ASIC to read out the Advanced Implantation Detector Array for experiments in nuclear decay spectroscopy
D.Braga *et al.*
<https://dx.doi.org/10.1109/ANIMMA.2011.6172853>

Acknowledgements

It is a pleasure to acknowledge the advice and help of many members of the CRYRING and NuCAR collaborations, in particular, Michael Lestinsky, Angela Braüning-Demian, Yuri Litvinov, Jan Glorius, René Reifarh, Nikolaos Petridis and Carsten Brandau.